ments without prior synaptic tetanization (Fig. 1B), robust LTD of about 30% was always apparent 1 min after the light tetanus. Thus, synaptically induced LTD occludes photostimulation LTD, suggesting similar mechanisms of expression of both kinds of LTD (*15*).

The mechanism of LTD induction is very quick. The reduction of the neuronal depolarizations was always apparent at the first stimulation, 1 min after the tetanus. It should therefore be mediated by a local, membrane-bound process. One possibility could be changed ion channel kinetics, but we obtained no evidence for this explanation. Another explanation could be a modulation of glutamate channel conductance (*16*).

The method of infrared-guided laser stimulation allows the stimulation of selected target points on neurons with a spatial precision of 10 μm. Neurons can be depolarized by light flashes with a duration of a few milliseconds for at least 1 hour without any signs of photodamage. The use of infrared videomicroscopy for the visualization of neurons obviates the necessity of neuronal staining by fluorescent dyes (*17*) or biocytin (*18*), which have inherent drawbacks.

LTD is spatially restricted. Tetanic activation of postsynaptic glutamate receptors by photolysis alone can induce LTD. This postsynaptic LTD of glutamate receptors is sufficient to account for the LTD of EPSPs seen 30 min after electrical stimulation of afferent fibers. The LTD of a small membrane patch (Fig. 2C) suggests that, during synaptic transmission, a few or even single synapses may undergo LTD in isolation. These results are compatible with observations that single spines show transient $[Ca^{2+}]$ increases after synaptic stimulation (*19*).

In conclusion, our experiments indicate the importance of the postsynaptic site for the generation of LTD. At this site, LTD can be induced very quickly and with high precision. Our finding of high spatial specificity would allow for a model of fine tuning of the transmission strength of each individual synapse, depending on its input. Such a specific mechanism would be very attractive for "high-density storage" of memory traces.

References and Notes

1. R. W. Tsien and R. Malinow, *Cold Spring Harbor Symp. Quant. Biol.* **55**, 147 (1990); T. Manabe, P. Renner, R. A. Nicoll, *Nature* **355**, 50 (1992).
2. G. S. Lynch, V. K. Gribkoff, S. A. Deadwyler, *Nature* **263**, 151 (1976); S. N. Davies, R. A. J. Lester, K. G. Reymann, G. L. Collingridge, *ibid.* **338**, 500 (1989); R. J. Cormier, M. D. Mauk, P. T. Kelly, *Neuron* **10**, 907 (1993).
3. T. V. P. Bliss and M. S. Fazeli, in *Cortical Plasticity*, M. S. Fazeli and G. L. Collingridge, Eds. (BIOS Scientific, Oxford, UK, 1996), pp. 61–82.
4. K. Kandler, L. C. Katz, J. A. Kauer, *Nature Neurosci.* 1, 119 (1998).
5. The gradient contrast system (GC) we developed gives images of neurons similar to images obtained with differential interference contrast but with superior contrast and light intensity. As in the GC system (Luigs and Neumann), no optical elements for contrast generation had to be placed behind the objective (60×, 0.9 numerical aperture, Olympus); the full power of the UV laser light can reach the neuron. The light of the UV laser was focused through the microscope objective to an optical spot of 1-μm diameter. The power of the laser (Enterprise II, Coherent) was adjusted with its remote control to 5 to 10 mW to evoke a depolarizing response of about 3 to 5 mV at the soma in response to 3-ms shuttered light pulses (Uniblitz shutter; Vincent Associates). Glutamate was applied by photolysis (wavelength = 351 to 364 nm) of γ-(α-carboxy-2-nitrobenzyl) (CNB)–caged glutamate (Molecular Probes) added at a concentration of 0.25 to 0.5 mM to the superfusion solution, which was oxygenated in a recirculation system. No indications for effects of spontaneously hydrolyzed γ-CNB–caged glutamate were found. All photostimulation experiments were started at least 15 min after the addition of caged glutamate and TTX.
6. Parasaggital slices of the parietal neocortex (300 μm thick) from 14- to 21-day-old Sprague-Dawley rats were prepared according to standard procedures (*20*). The brain slices were placed in the recording chamber of the "infrapatch" setup (Luigs and Neumann) and superfused with solutions containing the following: 125 mM NaCl, 2.5 mM KCl, 1.25 mM NaH_2PO_4, 2 mM $CaCl_2$, 1 mM $MgCl_2$, 25 mM $NaHCO_3$, and 25 mM glucose (pH 7.38; 20° to 22°C). Whole-cell recordings from visually identified somata of layer V pyramidal neurons were made with a standard intracellular amplifier (npi) in bridge mode. Patch-clamp electrodes with open-tip resistances of 4 to 7 megaohms were used that contained the following: 130 mM K-gluconate, 5 mM KCl, 0.5 mM EGTA, 2 mM Mg-adenosine triphosphate, 10 mM Hepes, and 5 mM glucose (pH 7.2) (*21*). Data were stored and analyzed with a Macintosh-based recording system and standard software (Pulse, HEKA).
7. The supplementary figure can be found at www.sciencemag.org/feature/data/1043873.shl
8. M. B. Dalva and L. C. Katz, *Science* **265**, 255 (1994).
9. H. S. Swartzwelder, C. C. Ferrari, W. W. Anderson, W. A. Wilson, *Neuropharmacology* **28**, 441 (1989).
10. R. M. Mulkey and R. C. Malenka, *Neuron* **9**, 967 (1992); S. Bröcher, A. Artola, W. Singer, *Proc. Natl. Acad. Sci. U.S.A.* **89**, 123 (1992).
11. T. Bonhoeffer, V. Staiger, A. Aertsen, *Proc. Natl. Acad. Sci. U.S.A.* **86**, 8113 (1989).
12. G. Kunz, W. Kirsche, J. Wenzel, E. Winkelmann, H. Neumann, *Z. Mikrosk.-Anat. Forsch.* **3**, 396 (1972).
13. U. Staubli and G. Lynch, *Brain Res.* **513**, 113 (1990).
14. A. Baude *et al.*, *Neuroscience* **69**, 1031 (1995); R. C. Carroll *et al.*, *Nature Neurosci* **2**, 454 (1999).
15. H. Lee, K. Kameyama, R. L. Huganir, M. F. Bear, *Neuron* **21**, 1151 (1998).
16. T. A. Benke, A. Lüthi, J. T. R. Isaac, G. L. Collingridge, *Nature* **393**, 793 (1998).
17. S. H. Wang and G. J. Augustine, *Neuron* **15**, 755 (1995); J. Schiller, Y. Schiller, D. E. Clapham, *Nature Neurosci.* **1**, 114 (1998).
18. L. C. Katz and M. B. Dalva, *J. Neurosci. Methods* **54**, 205 (1994).
19. R. Yuste and W. Denk, *Nature* **375**, 682 (1995).
20. H.-U. Dodt, A. Frick, K. Kampe, W. Zieglgänsberger, *Eur. J. Neurosci.* **10**, 3351 (1998).
21. M. Andreasen and J. J. Hablitz, *J. Neurophysiol.* **72**, 326 (1994).
22. D. L. Petit, S. H. Wang, K. R. Gee, G. L. Augustine, *Neuron* **19**, 465 (1997).

23. We thank K. Lee for comments on this manuscript. Supported by a grant from the Sonderforschungsbereich 391.

22 June 1999; accepted 27 August 1999

Regulation of Intestinal α-Defensin Activation by the Metalloproteinase Matrilysin in Innate Host Defense

Carole L. Wilson,[1]* Andre J. Ouellette,[2,3] Donald P. Satchell,[2] Tokiyoshi Ayabe,[2] Yolanda S. López-Boado,[1] Jennifer L. Stratman,[1] Scott J. Hultgren,[4] Lynn M. Matrisian,[5] William C. Parks[1]

Precursors of α-defensin peptides require activation for bactericidal activity. In mouse small intestine, matrilysin colocalized with α-defensins (cryptdins) in Paneth cell granules, and in vitro it cleaved the pro segment from cryptdin precursors. Matrilysin-deficient ($MAT^{-/-}$) mice lacked mature cryptdins and accumulated precursor molecules. Intestinal peptide preparations from $MAT^{-/-}$ mice had decreased antimicrobial activity. Orally administered bacteria survived in greater numbers and were more virulent in $MAT^{-/-}$ mice than in $MAT^{+/+}$ mice. Thus, matrilysin functions in intestinal mucosal defense by regulating the activity of defensins, which may be a common role for this metalloproteinase in its numerous epithelial sites of expression.

One role of the mucosal epithelium is to function as an active barrier against the external environment. Secretion of antibiotic peptides by epithelial cells appears to be an important component of innate immunity (*1*). The α- and β-defensins comprise a family of cationic peptides that kill bacteria by membrane disruption (*2*, *3*). Granulocytes and several epithelial tissues (*4*), including the Paneth cells of the small intestine of most mammals (*3*, *5*, *6*), produce α-defensins as prepropeptides. In mice, Paneth cell α-defensins are termed cryptdins (crypt defensins) (*5*–*7*), of which six distinct peptides have been iso-

lated and characterized (*6*). Cryptdins and other antimicrobial molecules (lysozyme and secretory phospholipase A2) are released from secretory granules in response to bacteria or cholinergic agents (*6*, *8*). The pro segment of cryptdins maintains them in an inactive state (*9*); the protease that mediates removal of the pro domain, thereby regulating the level of functional peptides, has not been identified.

Previously, we showed that mRNA for matrilysin (MMP-7), a matrix metalloproteinase (MMP), localizes to Paneth cells in mice harboring a conventional microflora (*10*). Matrilysin expression parallels that of the cryptdins (*11*) in that it is produced postnatally and is abundant in the unchallenged adult animal (*10*). Rather than being secreted basally, matrilysin is released at the apical cell surface and is detectable within the crypt lumen (*12*) (Fig. 1A). No staining for matrilysin was observed in Paneth cells of matrilysin-deficient ($MAT^{-/-}$) mice (Fig. 1B). $MAT^{+/+}$ and $MAT^{-/-}$ crypts exhibited identical staining patterns for cryptdin-1, indicating that the absence of matrilysin does not affect cryptdin precursor expression (Fig. 1, C and D). Other MMPs expressed in the mouse small intestine, including collagenase-3 (MMP-13) and stromelysin-2 (MMP-10), were not seen in Paneth cells of $MAT^{+/+}$ animals (*13*).

Matrilysin prefers a leucine-arginine dipeptide sequence in the right-hand (P_1' and P_2') position of cleavage sites (*14*). The NH_2-terminal residue of cryptdins 1 to 3, 5, and 6 is a leucine, and, as deduced from the cDNA sequences, this amino acid is predicted to be the NH_2-terminal residue in all cryptdin family members (*15*) (Fig. 2A). Except for cryptdin-5, all cryptdin genes code for an arginine immediately after the NH_2-terminal leucine in the mature peptide (*15*). Finally, matrilysin itself does not have antimicrobial activity (*16*), supporting a role for it in procryptdin processing.

To address this possibility, we tested the ability of activated human matrilysin to cleave the pro segment from recombinant cryptdin precursors. At a 1:2 molar ratio of enzyme to substrate, a ratio typically used in MMP-substrate reactions in vitro (*17*), purified procryptdin-1 (PC-1) (*18*) was converted to mature cryptdin-1 (Fig. 2B). This reaction was inhibited by EDTA, a chelator of metal ions required for MMP activity (Fig. 2B). Peptide sequencing confirmed that matrilysin cleaved PC-1 to produce authentic cryptdin-1 with an NH_2-terminal sequence of LRDLV (*19*). To test if matrilysin recognizes heterologous cryptdin precursors, we expressed a procryptdin chimera (proCC) (*18*) consisting of procryptdin-15 sequence, the last three COOH-terminal residues of cryptdin-4 (PRR), and a 6xHis tag (Fig. 2A). proCC was also efficiently cleaved by matrilysin (Fig. 2B), and NH_2-terminal amino acid sequencing verified that catalysis occurred at the same position as in PC-1. Increasing the molar concentration of substrate reduced the amount of

[1]Department of Pediatrics, Division of Allergy and Pulmonary Medicine, Washington University School of Medicine, St. Louis, MO 63110, USA. [2]Department of Pathology and [3]Department of Microbiology and Molecular Genetics, College of Medicine, University of California, Irvine, CA 92697, USA. [4]Department of Molecular Microbiology and Microbial Pathogenesis, Washington University School of Medicine, St. Louis, MO 63110, USA. [5]Department of Cell Biology, Vanderbilt University School of Medicine, Nashville, TN 37232, USA.

*To whom correspondence should be addressed. E-mail: wilson_c@kids.wustl.edu

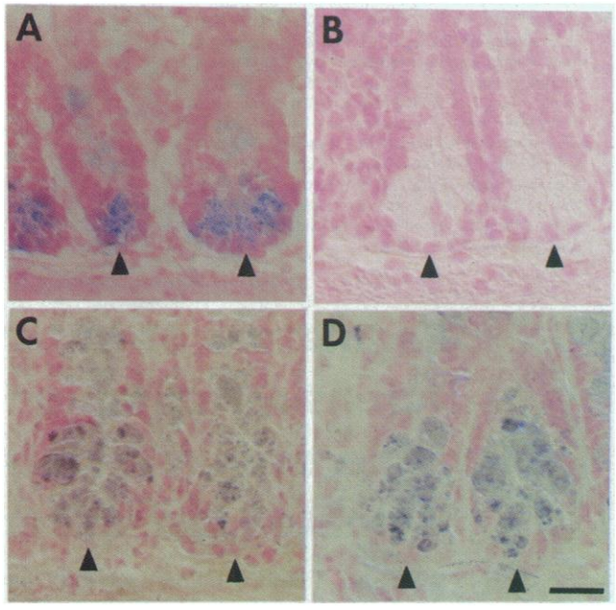

Fig. 1. Immunolocalization of matrilysin and cryptdin-1 in $MAT^{+/+}$ and $MAT^{-/-}$ small intestinal crypts. Frozen sections of small intestine from $MAT^{+/+}$ (**A** and **C**) and $MAT^{-/-}$ (**B** and **D**) mice were stained with polyclonal antibodies against matrilysin (*20*) (A and B) and cryptdin-1 (*7*) (C and D) as described (*12*). The blue indicates positive staining; red staining identifies the nuclei. Arrowheads indicate clusters of Paneth cells at the base of adjacent crypts. Photographs were taken with Nomarski optics. Scale bar, 25 μm.

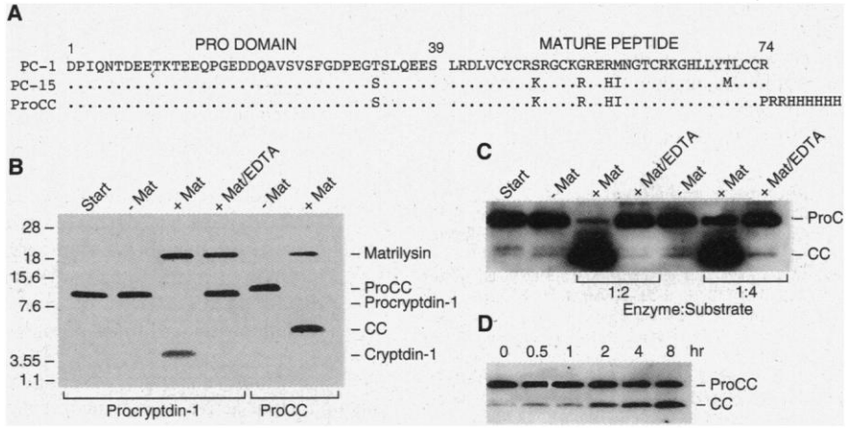

Fig. 2. Cleavage of cryptdin precursors by matrilysin. (**A**) The amino acid sequence alignment of procryptdin-1 (PC-1), procryptdin-15 (PC-15), and the recombinant procryptdin chimera (proCC) is shown. Dots denote residues of identity with PC-1. Residues 40 and 41 are the known or deduced NH_2-terminal amino acids of processed cryptdins. (**B**) One microgram each of PC-1 and proCC (*18*) was incubated for 24 hours with 1 μg of catalytically active recombinant human matrilysin (+Mat) (Chemicon) in assay buffer [10 mM Hepes (pH 7.4), 0.15 M NaCl, and 5 mM $CaCl_2$] with or without 50 mM EDTA. Reactions were analyzed by tris-tricine SDS-PAGE (15% polyacrylamide). Proteins were visualized by staining the gel with GelCode Blue reagent (Pierce), which does not detect the pro segment. The legend to the right of the gel identifies the bands corresponding to matrilysin, the precursors PC-1 and proCC, and their cleavage products cryptdin-1 and CC, respectively. CC migrates less rapidly than cryptdin-1 because of the additional residues from cryptdin-4 and the 6xHis tag. (**C**) Matrilysin digestion of proCC was set up as in (B), but the molar ratio of enzyme to substrate was varied as indicated. After tris-tricine SDS-PAGE, proteins were transferred to polyvinylidene difluoride (PVDF) membrane, and reaction products (proCC and CC) were detected with an antibody to His (COOH-terminal) (Invitrogen) at a 1:5000 dilution. (**D**) A time course of proCC cleavage by matrilysin was analyzed as in (C).

proCC converted to CC peptide (Fig. 2C). Although only 50% of the precursor was cleaved by 8 hours (Fig. 2D), the in vitro reaction kinetics may not reflect the in vivo rate.

$MAT^{-/-}$ mice were used to explore the relation between matrilysin expression and processing of cryptdin precursors in vivo. When housed under specific pathogen-free conditions, these mice do not develop spontaneous infections by opportunistic microorganisms. In addition, expression of cryptdin genes is normal in $MAT^{-/-}$ mice (*20*) (Fig. 1). To assess if procryptdin processing is altered in $MAT^{-/-}$ mice, we analyzed small intestinal extracts by acid-urea polyacrylamide gel electrophoresis (AU-PAGE). In this acidic gel system, cryptdin peptides are the most rapidly migrating of mouse intestinal peptides and separate in a predictable pattern according to their overall positive charge (*21*, *22*). Mature cryptdin peptides were present in $MAT^{+/+}$ mice (Fig. 3A, bracket); however, there was no evidence of processed cryptdins in intestinal extracts of $MAT^{-/-}$ animals (Fig. 3A) (*23*). Further analysis of $MAT^{-/-}$ extracts by reversed-phase high-performance liquid chromatography (rpHPLC) verified that peptides in $MAT^{+/+}$ samples eluting with retention times characteristic of cryptdins were absent from $MAT^{-/-}$ intestinal extracts (*13*). Finally, although both procryptdins and mature cryptdins were detected in isolated $MAT^{+/+}$ Paneth cell granules, only precursors were found in $MAT^{-/-}$ granules (*24*). In $MAT^{+/-}$ small intestine, processed peptide levels were equivalent to those in $MAT^{+/+}$ animals (*13*).

The lack of mature cryptdins in $MAT^{-/-}$ mice suggested that procryptdins would accumulate in these animals. Indeed, protein immunoblot analysis of intestinal extracts with an antibody against the cryptdin-1 pro domain (*25*) showed an increase in cryptdin pro forms in $MAT^{-/-}$ extracts (Fig. 3B). The immunoblot also confirmed that the absence of cryptdin peptides in $MAT^{-/-}$ animals is not due to diminished procryptdin synthesis. Together, the results demonstrate that processing of procryptdins in vivo is dependent on matrilysin and indicate that it occurs intracellularly. Furthermore, the observation that matrilysin cleaves the pro segment from cryptdin precursors in vitro suggests that this metalloenzyme directly activates procryptdins

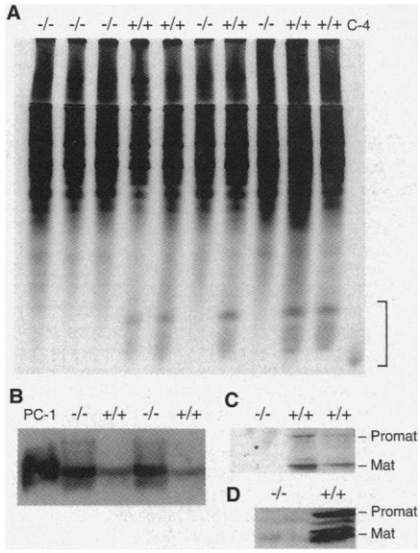

Fig. 3. Lack of procryptdin processing in $MAT^{-/-}$ small intestine. **(A)** Acetic acid extracts of small intestine were prepared and analyzed by AU-PAGE as described (*21*, *22*) without prior knowledge of genotype. Synthetic refolded cryptdin-4 (C-4), the most rapidly migrating of the mouse enteric defensins, was included in the gel as an α-defensin marker. The bracket indicates the position where mature cryptdins migrate. There was complete concordance between genotype and presence ($MAT^{+/+}$ lanes) or absence ($MAT^{-/-}$ lanes) of detectable peptides. A band comigrating with the cryptdin-4 marker is not readily detected in the extracts, as this peptide is the least abundant of the characterized cryptdins. **(B)** Lyophilized $MAT^{+/+}$ and $MAT^{-/-}$ intestinal extracts were dissolved in sample buffer, and equal amounts of protein were analyzed by tris-tricine SDS-PAGE (15% polyacrylamide). Recombinant PC-1 (0.5 μg) was included as a standard. Proteins were transferred to PVDF and immunoblotted with a polyclonal antibody against the pro segment of PC-1 (1:2000 dilution) (*25*). **(C)** Extracts from (B) were analyzed by SDS-PAGE (12% polyacrylamide) and immunoblotting with a polyclonal antibody against mouse matrilysin (*20*). The precursor (Promat) and mature (Mat) forms of matrilysin, at 28 kD and 19 kD, respectively, are indicated. **(D)** Granules isolated from 3500 crypts ($MAT^{+/+}$ and $MAT^{-/-}$) (*35*) were analyzed as in (C).

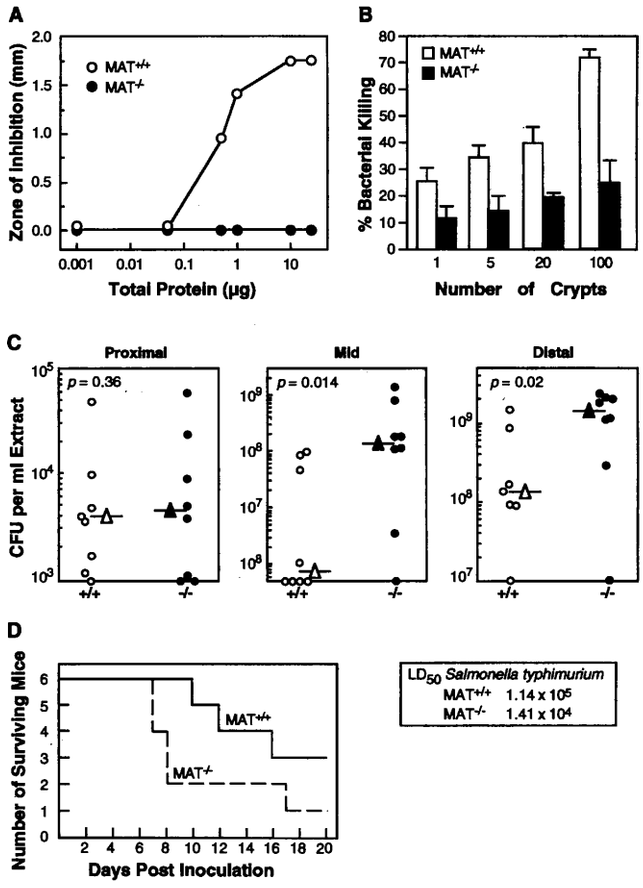

Fig. 4. Association of matrilysin deficiency with a decrease in microbicidal activity. **(A)** Total small intestinal protein extracts from $MAT^{+/+}$ and $MAT^{-/-}$ mice were dissolved at concentrations ranging from 0.3 to 8.3 μg/μl in sterile 0.01% acetic acid for performance of agar diffusion antibacterial assays (*22*). Three microliters of each solution was applied to wells in solidified agarose containing *E. coli* ML35. Antibacterial activity (zone of inhibition) was determined by subtracting the radius of the well from the total radius of the zone of clearance. The results shown here are representative of several independent experiments. **(B)** One thousand logarithmic-phase *S. typhimurium phoP* bacteria (*30*) (estimated by optical density at 620 nm) in isotonic PIPES buffer were combined with 5 μl of CCh-stimulated secretion supernatants from the indicated number of crypts (*29*). After incubation for 1 hour at 37°C with shaking, CFUs were determined by plating in triplicate on nutrient agar. The mean number of bacteria killed is expressed as a percentage (±SD) of controls from which crypts were omitted. $P \leq 0.01$ by Student's t test. **(C)** $MAT^{+/+}$ and $MAT^{-/-}$ mice were inoculated intragastrically with 1 to 2 × 10^{10} CFUs of *E. coli* KBC-236 and killed 2 hours later for small intestine extraction and quantification of surviving bacteria in the small intestine (*32*). The data were obtained from two separate experiments, with a total of seven to eight mice of each genotype. We calculated the median, or 50th, percentile (denoted by bisected triangles) and analyzed the statistical significance of the data using the nonparametric Wilcoxon/Mann-Whitney Rank Sum Test (one-tailed). **(D)** To assess mouse survival after oral challenge with a virulent strain of *S. typhimurium* (ATCC 14028s), we inoculated $MAT^{+/+}$ and $MAT^{-/-}$ females (C57BL/6 background) at about 6 weeks of age with 2.89 × 10^5 CFUs as described (*32*). LD_{50} values were determined with the moving average interpolation method (*33*).

in vivo as well, although potential intermediates in the processing pathway cannot yet be ruled out. The presence of the active form of matrilysin in small intestinal homogenates (*26*) and acid extracts (Fig. 3C) and within Paneth cell granules (Fig. 3D) supports MMP-mediated intracellular processing.

To assess the biological effect of cryptdin peptide deficiency, we determined the antimicrobial activity of small intestinal extracts in radial diffusion assays that measure combined bactericidal and bacteriostatic activity (*22*). At protein concentrations at which $MAT^{+/+}$ extracts showed maximal killing activity against *Escherichia coli* ML35, $MAT^{-/-}$ extracts were completely inactive (Fig. 4A). Zones of clearance with $MAT^{-/-}$ extracts were detected only with 100 μg of protein, a level 10 times as great as the highest $MAT^{+/+}$ concentration tested (*13*). In another approach, intact crypts were isolated from $MAT^{+/+}$ and $MAT^{-/-}$ small intestines (*27*), and Paneth cell degranulation was stimulated by the cholinergic agent carbamylcholine (CCh) (*28*, *29*). AU-PAGE confirmed the presence of defensins in supernatants from CCh-treated $MAT^{+/+}$ crypts; these peptides were absent in untreated supernatants (*24*). In a liquid-phase assay measuring bactericidal activity, $MAT^{-/-}$ crypt supernatants killed a defensin-sensitive strain of *Salmonella typhimurium* (*30*) less efficiently than $MAT^{+/+}$ supernatants, even at the single-crypt level (Fig. 4B). Although other Paneth cell components released upon degranulation likely contribute to the antibacterial activity of $MAT^{-/-}$ crypt supernatants, the reduced activity of these supernatants is consistent with a deficiency in functional cryptdins.

To ascertain the effects of cryptdin deficiency in vivo, we assessed the fate of exogenous bacteria in $MAT^{+/+}$ and $MAT^{-/-}$ small intestine. The indicator strain of bacteria, KBC-236, is a kanamycin-resistant *E. coli* derivative expressing type-1 adherent pili that mediate binding to mucosal epithelium (*31*). $MAT^{+/+}$ and $MAT^{-/-}$ mice were orally infected with KBC-236, and the number of viable microorganisms remaining in the small intestine was determined by growth on selective media (*32*). Because these bacteria are noninvasive in the intestine (*16*), in contrast to enteric pathogens such as *Salmonella*, they are particularly appropriate for quantification of bacterial survival. Infected mice were killed 2 hours after inoculation to minimize changes in bacterial numbers by cell division. The median number of viable KBC-236 recovered from the proximal small intestine, where Paneth cell density is relatively low, was about the same for both $MAT^{+/+}$ and $MAT^{-/-}$ mice (Fig. 4C) and represented only a small percentage of the input bacteria. In contrast, the median number of bacteria recovered from $MAT^{-/-}$ mid and distal segments was higher than that from $MAT^{+/+}$ mice (Fig. 4C). In both $MAT^{+/+}$ and $MAT^{-/-}$ mice, bacterial recovery increased from segment to segment along the proximal-distal axis, excluding the possibility that bacterial transit is altered in $MAT^{-/-}$ mice. In addition, little difference in bacterial numbers was noted at 30 min after inoculation, when the majority of bacteria were still in the proximal intestine (*13*). Thus, despite the presence of other antimicrobial molecules, survival of exogenous bacteria in the small intestine is enhanced in the absence of matrilysin. In addition, the oral 50% lethal dose (LD_{50}) (*33*) of a virulent, invasive strain of *S. typhimurium* for $MAT^{-/-}$ mice was one-tenth that for $MAT^{+/+}$ mice (Fig. 4D). $MAT^{-/-}$ mice succumbed more rapidly to *Salmonella* infection than did $MAT^{+/+}$ animals at a bacterial dose slightly above the LD_{50} for $MAT^{+/+}$ mice (Fig. 4D). Although we cannot exclude a potential matrilysin-dependent systemic mechanism, these results support our conclusion that epithelial expression of matrilysin is important in restricting bacterial colonization and access to the intestinal mucosa.

These findings show involvement of an MMP in host defense against bacteria and extend the activity of matrilysin beyond that of connective tissue remodeling. The absence of any defect in matrix turnover in $MAT^{-/-}$ mice and the ability of matrilysin to cleave nonmatrix substrates (*34*) support a role for this metalloenzyme in protein processing. The wide spectrum of constitutive matrilysin expression in different organs suggests that the enzyme has a common function among mucosal tissues. The role we have described for matrilysin in the small intestine, specifically regulation of defensin activation, may be the shared function of this metalloproteinase in other epithelia.

References and Notes

1. C. L. Bevins, *Ciba Found. Symp.* **186**, 250 (1994).
2. M. E. Selsted and S. S. Harwig, *J. Biol. Chem.* **264**, 4003 (1989).
3. T. Ganz, M. E. Selsted, R. I. Lehrer, *Eur. J. Haematol.* **44**, 1 (1990); T. Ganz and R. I. Lehrer, *Pharmacol. Ther.* **66**, 191 (1995); E. Martin, T. Ganz, R. I. Lehrer, *J. Leukocyte Biol.* **58**, 128 (1995); T. Ganz and J. Weiss, *Semin. Hematol.* **34**, 343 (1997); T. Ganz and R. I. Lehrer, *Curr. Opin. Immunol.* **10**, 41 (1998).
4. D. M. Svinarich, N. A. Wolf, R. Gomez, B. Gonik, R. Romero, *Am. J. Obstet. Gynecol.* **176**, 470 (1997); V. Grandjean, S. Vincent, L. Martin, M. Rassoulzadegan, F. Cuzin, *Biol. Reprod.* **57**, 1115 (1997); A. J. Quayle *et al.*, *Am. J. Pathol.* **152**, 1247 (1998).
5. P. B. Eisenhauer, S. S. Harwig, R. I. Lehrer, *Infect. Immun.* **60**, 3556 (1992).
6. A. J. Ouellette and M. E. Selsted, *FASEB J.* **10**, 1280 (1996); A. J. Ouellette, *Gastroenterology* **113**, 1779 (1997).
7. M. E. Selsted, S. I. Miller, A. H. Henschen, A. J. Ouellette, *J. Cell Biol.* **118**, 929 (1992).
8. Y. Satoh, K. Ishikawa, K. Ono, L. Vollrath, *Digestion* **34**, 115 (1986); Y. Satoh, *Cell Tissue Res.* **253**, 397 (1988); *ibid.* **251**, 87 (1988).
9. E. V. Valore, E. Martin, S. S. Harwig, T. Ganz, *J. Clin. Invest.* **97**, 1624 (1996).
10. C. L. Wilson, K. J. Heppner, L. A. Rudolph, L. M. Matrisian, *Mol. Biol. Cell* **6**, 851 (1995).
11. A. J. Ouellette *et al.*, *J. Cell Biol.* **108**, 1687 (1989).
12. For immunohistochemistry, frozen sections stored at −80°C were air dried and incubated in Bouin's fixative for 15 min at room temperature. After a phosphate-buffered saline (PBS) wash, endogenous peroxidases were quenched with 0.6% H_2O_2 in methanol for 15 min. Slides were rinsed in tris-buffered saline and then blocked for 1 hour in buffer [10 mM tris-HCl (pH 7.5), 0.1 M $MgCl_2$, 0.5% Tween-20, 1% bovine serum albumin (BSA), and 5% goat serum]. Sections were incubated overnight at 4°C with 1:5000 (antibody to matrilysin) or 1:1000 (antibody to cryptdin-1) dilutions of antibody in blocking solution. Sections were developed with the rabbit Vectastain Elite ABC kit (Vector Laboratories). Protein was visualized with True Blue substrate, and nuclei were counterstained with Contrast Red (Kirkegaard and Perry).
13. C. L. Wilson *et al.*, data not shown.
14. M. M. Smith, L. Shi, M. Navre, *J. Biol. Chem.* **270**, 6440 (1995).
15. A. J. Ouellette *et al.*, *Infect. Immun.* **62**, 5040 (1994).
16. Y. S. López-Boado and W. C. Parks, unpublished data.
17. K. Miyazaki, Y. Hattori, F. Umenishi, H. Yasumitsu, M. Umeda, *Cancer Res.* **50**, 7758 (1990); G. Murphy, M. I. Cockett, R. V. Ward, A. J. P. Docherty, *Biochem. J.* **277**, 277 (1991); A. Siri *et al.*, *J. Biol. Chem.* **270**, 8650 (1995).
18. For generation of recombinant PC-1, nucleotides +58 to +280 of PC-1 cDNA were amplified from a full-length clone with primers 5′-GCGCGAATTCA TCGAGGGAAGGATCCTATCCAAAACACA-3′ (forward cryptdin sequence underlined) and 5′-ATATATGTCGACTCAGCGACAGCAGAGCGTGTACAATAAATG-3′ (reverse cryptdin sequence underlined). PC-1 was expressed in *E. coli* as a fusion protein to maltose-binding protein with the pMalc2 expression vector (New England Biolabs). Bacteria were lysed in buffer containing 10 mM tris-HCl (pH 7.4), 200 mM NaCl, 1 mM EDTA, deoxyribonuclease I (50 μg/ml), 50 mM $MgCl_2$, and 30% (v/v) B-PER reagent (Pierce). The soluble fusion protein was purified by amylose resin affinity chromatography and subjected to Factor Xa digestion to liberate PC-1, which was further purified by C-18 rpHPLC on a Vydac 218TP510 column. Protein homogeneity was assessed by AU-PAGE (12.5% polyacrylamide) and tris-tricine SDS-PAGE (10 to 20% polyacrylamide gradient). To produce the chimeric procryptdin (proCC), we amplified preprocryptdin-15 cDNA from −42 to +274 with forward primer 5′-GCGGATCCATTGAGCTCCTGCTCA-3′ and reverse primer 5′-GGCCTAGGACAGCAGAGCGTGTACAATAAATG-3′. The reverse primer encoded a threonine residue substitution (characteristic of cryptdin-1) for the methionine normally at position 73 in procryptdin-15. A 40–base pair fragment encoding the last three COOH-terminal residues of cryptdin-4 (PRR) and the 6xHis tag was ligated to the amplified product before cloning into the baculovirus transfer vector pVL1393. Sf9 cells were transfected with this construct and BaculoGold DNA (Pharmingen) to produce recombinant baculovirus. After a single round of amplification, High Five insect cells (Stratagene) were infected and harvested 4 days later. Cell pellets were lysed in denaturing buffer [8 M urea, 100 mM sodium phosphate (pH 8), 10 mM tris-HCl (pH 8), and 1% Triton X-100] and clarified by passage through an 18-G needle and centrifugation. proCC was purified from the supernatant by nickel–nitrilotriacetic acid metal-affinity chromatography (Qiagen) and elution at low pH. Purity was assessed by tris-tricine SDS-PAGE and Coomassie blue staining.
19. Single-letter abbreviations for the amino acids are as follows: A, Ala; C, Cys; D, Asp; E, Glu; F, Phe; G, Gly; H, His; I, Ile; K, Lys; L, Leu; M, Met; N, Asn; P, Pro; Q, Gln; R, Arg; S, Ser; T, Thr; V, Val; W, Trp; and Y, Tyr.
20. C. L. Wilson, K. J. Heppner, P. A. Labosky, B. L. M. Hogan, L. M. Matrisian, *Proc. Natl. Acad. Sci. U.S.A.* **94**, 1402 (1997).
21. M. E. Selsted and H. W. D. Becker, *Anal. Biochem.* **155**, 270 (1986).
22. M. E. Selsted, *Genet. Eng.* **15**, 131 (1993).
23. The difference between $MAT^{+/+}$ and $MAT^{-/-}$ cryptdin peptide profiles was consistently seen in four

independent, blind analyses with extracts from over 30 animals. Neither the genetic background of the mice (C57BL/6 or 129/Sv-C57BL/6 hybrid) nor the housing environment (barrier facilities at Vanderbilt University and Washington University) affected the results.
24. T. Ayabe and A. J. Ouellette, unpublished data.
25. Residues 1 to 39 of the cryptdin-1 pro segment (Fig. 2A) were deduced from cDNA sequence (*15*). The peptide was synthesized in solid phase and purified to homogeneity by rpHPLC by Quality Controlled Biochemicals (Hopkinton, MA). The sequence was verified by mass spectrometry and amino acid analysis. After conjugation of the peptide to BSA, polyclonal antiserum to pro segment was produced in a sheep by administration of three to four dorsal subcutaneous injections of BSA-conjugated peptide mixed with an equal volume of complete Freund's adjuvant. Injections were repeated twice, and the antiserum titer was evaluated by enzyme-linked immunosorbent assay by Quality Controlled Biochemicals. The antibody also recognizes proCC, suggesting that it is immunoreactive against multiple procryptdins. The pro segment sequence is highly conserved among the family.
26. R. L. Shattuck-Brandt, L. W. Lamps, K. J. Heppner Goss, R. N. DuBois, L. M. Matrisian, *Mol. Carcinog.* **24**, 177 (1999).
27. D. Darmoul and A. J. Ouellette, *Am. J. Physiol.* **271**, G68 (1996); D. F. Cano-Gauci *et al.*, *Exp. Cell Res.* **208**, 344 (1993).
28. Y. Satoh, Y. Habara, K. Ono, T. Kanno, *Gastroenterology* **108**, 1345 (1995).
29. Crypts were isolated from MAT$^{+/+}$ and MAT $^{-/-}$ males (original 129/Sv-C57BL/6 hybrid backcrossed to C57BL/6 for 10 generations) as described (*27*). Eluted crypts resuspended in ice-cold Ca^{2+}- and Mg^{2+}-free Hank's balanced salt solution were transferred singly to siliconized microcentrifuge tubes to obtain 1, 5, or 20 crypts per tube; to transfer 100 crypts per tube, we measured crypt numbers with a hemacytometer and transferred appropriate volumes. Crypts were centrifuged at 700*g* for 5 min and resuspended in 30 μl of isotonic PIPES buffer [10 mM PIPES (pH 7.4) and 0.8% NaCl] containing 100 μM CCh to stimulate selectively Paneth cell degranulation (*28*). After a 30-min incubation at 37°C in a rotary shaker at 150 cycles/min, crypts were centrifuged for 5 min at 700*g*, and supernatants containing CCh-induced Paneth cell secretions were harvested aseptically and stored at −20°C.
30. A. J. Ouellette, S. I. Miller, A. H. Henschen, M. E. Selsted, *FEBS Lett.* **304**, 146 (1992).
31. S. J. Hultgren *et al.*, *Cell* **73**, 887 (1993).
32. Male and female MAT$^{+/+}$ and MAT$^{-/-}$ mice (C57BL/6 background) were infected at 5 weeks of age. *Escherichia coli* KBC-236 (in 150 ml of Luria-Bertani broth containing ampicillin and kanamycin) was grown statically for 48 hours at 37°C to induce pili formation. Bacteria were pelleted by centrifugation at 10,000 rpm for 10 min and washed with cold sterile PBS. After recentrifugation, bacteria were resuspended in 1.5 ml of PBS, and the approximate concentration of bacteria was determined by optical density at 600 nm. The actual number of colony-forming units (CFUs) was measured by plating serial dilutions. Mice were made to fast for 2 hours before oral administration of bacteria. Animals were lightly anesthetized with methoxyfluorane and then given a 0.1-ml dose of 0.1 M sodium bicarbonate (to neutralize stomach acids) immediately followed by a 0.1-ml bolus of bacteria (1 to 2 × 10^{10} CFUs) in PBS with a 1-ml syringe fitted with a stainless steel feeding needle. Mice were given access to food 30 min after inoculation. After 2 hours, mice were anesthetized and killed by cervical dislocation. The small intestine was removed en bloc and cut into three portions of equal length (proximal, mid, and distal segments). Each segment was homogenized in 3 ml of PBS and serially diluted for plating on kanamycin for determination of CFUs per milliliter.
33. S. C. Gad and C. S. Weil, in *Principles and Methods of Toxicology*, A. W. Hayes, Ed. (Raven, New York, 1989), pp. 463–467; S. Welkos and A. O'Brien, *Methods Enzymol.* **235**, 29 (1994).
34. A. J. H. Gearing *et al.*, *Nature* **370**, 555 (1994); P. A. Marcotte, I. M. Kozan, S. A. Dorwin, J. M. Ryan, *J. Biol. Chem.* **267**, 13803 (1992).
35. Paneth cell secretory granules were prepared from enriched crypt fractions from duodenum and ileum. Crypts dissociated from the lamina propria with EDTA (*27*) were resuspended in ice-cold Ca^{2+}- and Mg^{2+}-free Hank's balanced salt solution, and cells were lysed in a Parr cavitation bomb. After an initial centrifugation of cell lysate at 700*g*, granules were pelleted from the supernatant at 27,000*g* for 40 min.
36. We thank R. P. Mecham, T. J. Broekelmann, and A. H. Henschen for protein sequencing; M. E. Selsted for the antibody to cryptdin-1, the cryptdin-4 peptide standard, and helpful discussions; M. A. Mulvey for help with bacteria and critical review of the manuscript; F. Heffron for the virulent *S. typhimurium* strain 14028s; and S. Shapiro and J. Lohi for insightful comments on the manuscript. All animal experiments were performed with the approval of the Washington University School of Medicine Animal Studies Committee. This work was supported by a Barnes-Jewish Hospital Foundation grant (to C.L.W.) and by grants from NIH (to W.C.P., A.J.O., L.M.M., and S.J.H.).

7 May 1999; accepted 20 August 1999

Est1 and Cdc13 as Comediators of Telomerase Access

Sara K. Evans and Victoria Lundblad*

Cdc13 and Est1 are single-strand telomeric DNA binding proteins that contribute to telomere replication in the yeast *Saccharomyces cerevisiae*. Here it is shown that fusion of Cdc13 to the telomerase-associated Est1 protein results in greatly elongated telomeres. Fusion proteins consisting of mutant versions of Cdc13 or Est1 confer similar telomere elongation, indicating that close physical proximity can bypass telomerase-defective mutations in either protein. Fusing Cdc13 directly to the catalytic core of telomerase allows stable telomere maintenance in the absence of Est1, consistent with a role for Est1 in mediating telomerase access. Telomere length homeostasis therefore is maintained in part by restricting access of telomerase to chromosome termini, but this limiting situation can be overcome by directly tethering telomerase to the telomere.

In most species, telomeres are composed of G-rich repetitive sequences that are elongated by telomerase (*1*). Several factors govern the balance between sequence addition and loss to maintain telomeres at a stable length, including positive and negative regulation of telomerase access to the chromosome terminus (*2–4*). In *S. cerevisiae*, five genes are required for the telomerase pathway (*4–7*). *TLC1* and *EST2* encode the RNA and reverse transcriptase subunits of telomerase, respectively, and as expected for subunits that are essential for catalysis, telomerase activity is absent in extracts from strains defective in *EST2* or *TLC1*(*7–9*). In contrast, mutations in *EST1*, *EST3*, and *CDC13* do not eliminate enzyme activity in vitro (*9*, *10*), despite the fact that strains carrying mutations in any of these three genes have the same severe telomere replication defect as *est2*-Δ or *tlc1*-Δ strains (*6*, *10*).

Both Cdc13 and Est1 bind single-strand telomeric DNA (*4*, *11*, *12*), although they make separate contributions to telomere replication and stability. Est1 is required solely for the telomerase pathway (*11*), whereas Cdc13 has an essential function at the telomere, presumably in protecting the end of the chromosome (*13*), as well as a role in telomere replication (*4*). This latter activity was revealed by a telomerase-defective allele of Cdc13, called *cdc13^{est}* [originally named *est4* (*6*)], leading to the proposal that Cdc13, like Est1, mediates telomerase access (*4*). The two proteins also display different biochemical properties. Est1, but not Cdc13, requires a free single-strand 3′ terminus for DNA binding and binds telomeric DNA with a 500-fold reduced affinity compared with Cdc13 (*4*, *11*). In addition, Est1 is associated with telomerase, whereas Cdc13 does not exhibit a detectable interaction with the enzyme (*14*).

These results suggest that telomerase is recruited to the telomere due to a direct (but weak) protein-protein interaction between Cdc13 and the enzyme, and the telomere shortening in the *cdc13^{est}* mutant strain is due to a further reduction in this interaction. This model predicts that increasing the association between Cdc13 and telomerase would increase telomere length. To test this, we examined the consequences of fusing Cdc13 to the telomerase-associated protein Est1 (*15*). Introduction of the gene encoding this Cdc13-Est1 fusion, present on a single-copy plasmid and expressed by the *CDC13* promoter, into a *CDC13*$^{+}$ strain resulted in substantial telomere elongation (Fig. 1A, lanes 2

Department of Molecular and Human Genetics, and Verna and Marrs McLean Department of Biochemistry, Baylor College of Medicine, Houston, TX 77030, USA.

*To whom correspondence should be addressed: E-mail: lundblad@bcm.tmc.edu